Journal of Chromatography A, 1218 (2011) 4104–4116

Contents lists available at ScienceDirect

Journal of Chromatography A

journal homepage: www.elsevier.com/locate/chroma

Review

Asymmetrical flow field-flow fractionation technique for separation and characterization of biopolymers and bioparticles

G. Yohannes, M. Jussila, K. Hartonen, M.-L. Riekkola *

Laboratory of Analytical Chemistry, Department of Chemistry, P.O. Box 55, FIN-00014, University of Helsinki, Finland

ARTICLE INFO

Article history:
Available online 18 January 2011

Keywords:
Asymmetrical flow field-flow fractionation
Biopolymers
Bioparticles
Macromolecules
Separation
Characterization

ABSTRACT

Field-flow fractionation (FFF) is one of the most versatile separation techniques in the field of analytical separation sciences, capable of separating macromolecules in the range 10^3–10^{15} g mol^{-1} and/or particles with 1 nm–100 μm in diameter. The most universal and most frequently used FFF technique, flow FFF, includes three types of techniques, namely symmetrical flow FFF, hollow fiber flow FFF, and asymmetrical flow FFF which is most established variant among them. This review provides a brief look at the theoretical background of analyte retention and separation efficiency in FFF, followed by a comprehensive overview of the current status of asymmetrical flow FFF with selected applications in the field of biopolymers and bioparticles.

Contents

1. Introduction

Field-flow fractionation (FFF) is one of the most versatile separation techniques in the field of analytical separation sciences, capable of separating macromolecular colloidal and particulate materials [1]. In 1966, Giddings first introduced the concept of field-flow fractionation (FFF) [2]. Since then, various subtechniques of FFF emerged. The major subtechniques are sedimentation FFF, thermal FFF, electric FFF, and flow FFF. In all the FFF subtechniques, sample separation is performed inside a narrow ribbon-like channel. The different techniques of FFF and their applications have been exhaustively described in general reviews [1,3–11]. Briefly, most of the FFF subtechniques have a channel with typical dimensions of 20–50 cm in length, 2–3 cm in width, and 0.01–0.05 cm in thickness. From the inlet, carrier liquid is pumped along the channel, establishing a parabolic flow profile (laminar Newtonian flow) moving the analytes towards the outlet. An external force field is

* Corresponding author. Tel.: +358 9 191 50268; fax: +358 9 191 50253.
E-mail addresses: marja-liisa.riekkola@helsink.fi, marja-liisa.riekkola@helsinki.fi (M.-L. Riekkola).

0021-9673/$ – see front matter © 2011 Elsevier B.V. All rights reserved.
doi:10.1016/j.chroma.2010.12.110

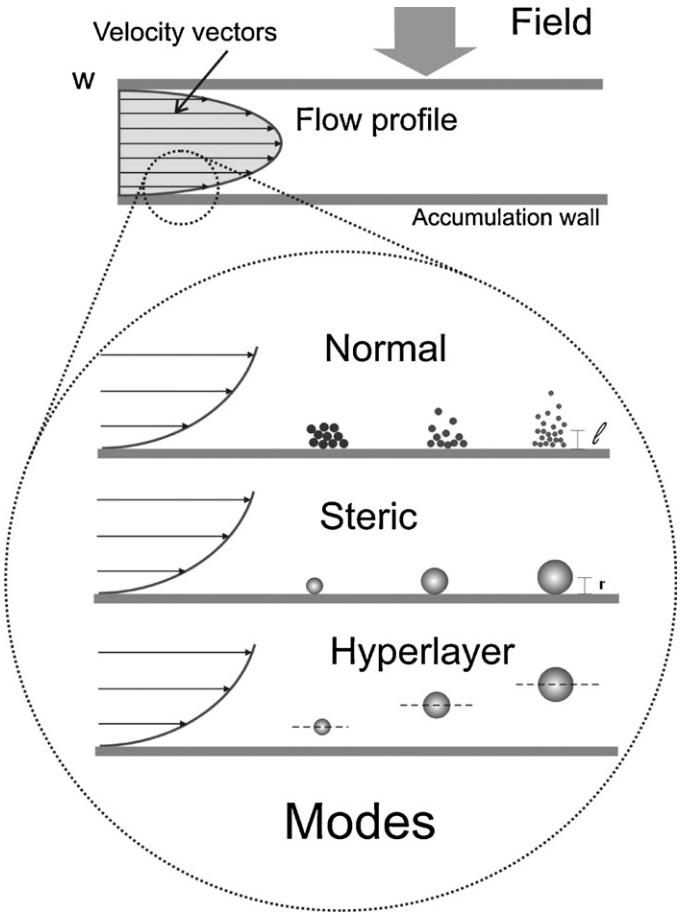

Fig. 1. Basic separation principle of field flow fractionation.

applied perpendicularly to the direction of the carrier liquid flow, forcing the sample components to accumulate towards the channel wall, termed accumulation wall (Fig. 1). Depending on the field applied (centrifugal, thermal, electrical, and hydrodynamic), each of the FFF subtechniques has different separation mechanism. Separation range for biopolymers is from 10^3 up to 10^{15} g mol^{-1} and that for bioparticles from 2 nm to 50 μm in diameter.

Flow field-flow fractionation (FlFFF), introduced in 1976 has proven to be the most universal and most frequently used of all FFF techniques [12]. The universality comes from the fact that the technique employs a hydrodynamic field applied by means of a secondary flow (cross flow) of carrier liquid perpendicular to the main flow [13]. Specifically, pumping a bulk liquid into the channel through one of the porous walls creates a convective flux. The liquid then exits the channel through the opposite wall, the so called "accumulation wall", that consists of a membrane placed on the top of a porous wall. For this reason, retention time in FlFFF is, in principle, dependent on diffusive flux, and the separation of macromolecules or particles occurs solely on the basis of differences in diffusion coefficients [12]. There are two main types of flow FFF: symmetrical flow FFF and asymmetrical flow FFF. In addition, some variant techniques exist, such as hollow fiber FlFFF (HFFlFFF). In the case of HFFlFFF, the field is radial with the cross flow radiating outwards over the entire inner surface of the tube while the rest of the liquid makes the channel flow.

The symmetrical flow FFF (FlFFFF) channel consists of upper and lower semi-permeable porous frits within the external blocks. When sample materials are introduced to a symmetrical FlFFF channel, they are pushed towards one side of channel wall (accumulation wall) by the applied field (cross flow). The main channel flow is stopped during the relaxation period for the time needed for the cross flow pump to deliver about one channel volume. During this short period of time, sample components find equilibrium positions where the field force and the diffusion are counterbalanced, and the sample components are differentially distributed along the channel cross section/thickness according to their sizes.

In the asymmetrical flow field-flow fractionation (AsFlFFF) the upper wall of the symmetrical flow FFF channel is replaced by an impermeable glass plate. The bottom channel plate is permeable, and made of a porous frit material (Fig. 1). AsFlFFF was first introduced by Wahlund and Giddings [14]. It was optimized further in the late eighties and the beginning of nineties [15–19]. In AsFlFFF, the cross flow is generated directly inside the channel, where the main flow coming from the inlet is divided to generate a cross flow through a semi-permeable membrane that is located in the bottom wall, while the rest of the longitudinal flow stream is directed to the detector(s). The membrane pore size in AsFlFFF is selected in such a way that only the solvent can pass through while the sample particles are retained (Fig. 2). In AsFlFFF, the relaxation process is called relaxation-focusing, i.e. the carrier liquid is allowed to flow in from both the inlet and outlet of the channel and meet at one point, the so-called focusing point. During this relaxation-focusing period sample migration is temporarily halted for achieving equilibrium after sample injection.

The focus of this review is on recent advances in asymmetrical flow field-flow fractionation. Selected examples that illustrate the benefits of AsFlFFF in the separation and the characterization of biopolymers and bioparticles hopefully accelerate future the exploitation of the technique.

2. Theoretical background in analyte retention

The theory of FlFFF applies almost directly to AsFlFFF, and it has been described in detail in many publications [6,12–14]. Hence, it will be described only briefly here. Two or three types of retention modes can be utilized within the same channel, namely normal (Brownian) and steric/hyperlayer (Figs. 1 and 2). After sample injection, the sample molecules are distributed homogeneously across the channel thickness (w), and are being pushed towards the bottom of the channel by the applied external, hydrodynamic force field. Finally, an exponential concentration distribution at the accumulation wall is built up. Since the accumulation wall acts as a barrier to the particles, the net movement of the sample species towards the external field is caused by diffusion from an area of high concentration at the accumulation wall to an area with lower concentration. After a certain relaxation period, a dynamic steady state is reached. A dimensionless retention parameter λ is defined as a ratio of l (the average distance between the sample particle and the channel wall) to w. For FlFFF λ is related to diffusion coefficient D of the sample particle, channel void volume V^0, cross flow rate $\dot{V}_c$, and w by:

$$\lambda = \frac{l}{w} = \frac{DV^0}{w^2\dot{V}_c} \quad (1)$$

In Eq. (1), V^0 and w are constants from the physical geometry of the channel, and $\dot{V}_c$ is the measurable volumetric flow rate. Separation of different particle zones in the channel is therefore based solely on the differences in diffusion coefficients of the particles [12]. Due to the parabolic flow profile, particles will migrate through the channel differentially according to their distance (l) from the accumulation wall. Smaller particles, which are located in the middle of the channel where the flow is faster, are eluted earlier. Larger particles are relatively closer to the accumulation wall and thus are eluted later. The retention ratio R, which is the ratio of the retention time t^0 of an unretained solute to the retention time

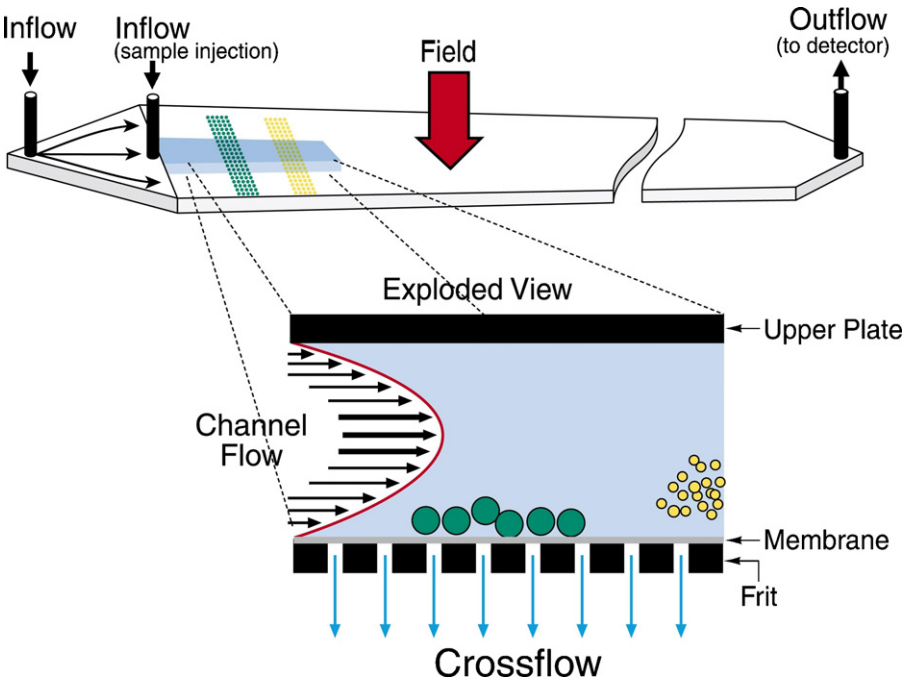

Fig. 2. Principle of the separation of biopolymer and bioparticle by AsFlFFF.
Reproduced with permission from Wyatt Technology Europe GmbH.

t_r of the retained solute, is dependent on λ according to:

$$R = \frac{t^0}{t_r} = 6\lambda\left[\coth\left(\frac{1}{2\lambda}\right) - 2\lambda\right] \quad (R \approx 6\lambda \quad \text{if} \quad \lambda < 0.1) \tag{2}$$

Using the Eqs. (1) and (2) as well as the Stokes expression for the diffusion coefficient, the hydrodynamic particle size d_H in flow FFF can be obtained as:

$$d_H = \frac{2kTV^0}{\pi\eta w^2 \dot{V}_c}\frac{t_r}{t^0} \tag{3}$$

When the particle size increases beyond a certain limit (approximately one micrometer), the hydrodynamic radius, r_H ($d_H = 2r_H$) in Eq. (3), becomes greater than the layer thickness l. Therefore Brownian motion becomes negligible and the external field holds particles firmly against the wall. The separation process is inverted, i.e. bigger particles emerge for detection before the smaller ones. The first mode of operation, which is affected by Brownian motion, is called the normal mode, whereas the second case is called a steric/hyperlayer mode.

3. Separation efficiency

As in chromatographic techniques, separation efficiency or band broadening is related to the plate height (H) or to the number of theoretical plates (N). Main factors affecting zone spreading in FFF are non-equilibrium (H_n), axial diffusion (H_D), instrumentation and operational effects (H_i), and sample polydispersity (H_p), via the relationship given in Eq. (4) [19–22]:

$$H = \frac{2D}{R\langle V\rangle} + \frac{\chi w^2\langle V\rangle}{D} + \sum_i H_i + H_p \tag{4}$$

where D is the diffusion coefficient of the particles, $\langle V\rangle$ is the average fluid velocity through the FFF channel, and χ is a non-equilibrium dimensionless parameter. The first term represents the contribution of the longitudinal diffusion and is generally negligible, because most analytes have high molar mass or size and consequently have a small diffusion coefficient. The second term is the contribution of non-equilibrium effect (H_n), where χ is a complicated function of λ. If λ is small, the approximation $\chi = 24\lambda^3$ can be used [23,24]. The third term is the sum of instrumental contributions (H_i) such as injection, detection, system dead volume, and flow irregularities [25–27]. For a well-constructed FFF apparatus that is being properly operated, the third term will also be small. The fourth term H_p is the contribution of polydispersity to the plate height [22]. The peaks for samples with wide particle size distribution are usually particularly broad because of the high selectivity of the FFF method.

4. Asymmetrical flow field-flow fractionation

AsFlFFF is the most universal FFF method today, and it has almost replaced the symmetrical version of FlFFF. It is well suitable for the separation and characterization of biopolymers and bioparticles, and it has found many applications in biology, industry, food and agricultural products, pharmaceuticals, biotechnology, and nanotechnology. Its wide applicability has been demonstrated in the characterization of analytes ranging from solutes with inherent molar masses of ~10^3 up to about 10^9 g mol^{-1}, and of particles with dimensions of <2 nm up to about 50 μm. The lower size limit is determined by the molecular weight cut-off of the membranes (~10^3 g mol^{-1}), whereas the upper size limit is assessed by a threshold of about 20% of the channel thickness, w [13].

While the conventional AsFlFFF utilizes a focusing/relaxation procedure that requires sample migration to be stopped for a period of time, the technique has been further developed to facilitate its use for biopolymer and bioparticle analysis without focusing/relaxation step. Frit inlet AsFlFFF (FI-AsFlFFF) was introduced to eliminate the focusing/relaxation procedure [28]. During sample injection in FI-AsFlFFF, sample components are pushed toward the accumulation wall by the action of a supplementary flow through a small permeable frit element located near the injection port. Thus the analytes are hydrodynamically relaxed while they are continuously carried to the separation process without stopping the migration. Other technologies, such as focus-flow

and slot outlet, provide special applications in AsFlFFF instruments [29]. With the slot outlet the carrier liquid (free of sample) above the sample layers is skimmed out so that only the concentrated sample goes to the detector. This is especially useful for bionalytical samples with low concentration to increase the detection sensitivity.

Miniaturized AsFlFFF channels have also been constructed with typical dimensions of 250–500 μm (thickness) × 9–11 cm (length) with a channel width of 7 mm at the sample inlet that tapers down to 3.5 mm at the channel outlet [30–32]. By scaling down the separation channel geometry, it is possible to achieve retention profiles in shorter time using less sample and carrier liquid (eluent). The resolution is similar in both miniaturized and conventional setup. In addition, both systems can be coupled to *n*LC–ESI-MS–MS [33].

5. Optimization of fractionation variables in asymmetrical flow field-flow fractionation

In AsFlFFF, almost any liquid solution (organic or aqueous solvent) can be used as mobile phase. The technique is highly flexible in terms of sample types, pH, ionic strength, and so on. It also provides a high selectivity in choosing flow rates, membrane types, and coupling to different types of detectors [34]. Although the AsFlFFF principle is simple, many operating parameters need to be optimized, such as the type of the membrane, the choice of elution solvent, ionic strength, pH, cross flow rate, working temperature, and injected mass. These parameters affect the degree of separation and sample recovery. Careful optimization leads to high recovery and good separation. Gimbert et al. [35] intensively reviewed the types of membranes, flow rates, carrier compositions, and detectors used in AsFlFF. For a comprehensive information, readers are referred to this contribution. Table 1 summarises the most recent optimized parameters applied in AsFlFlFF for the characterization of biopolymers and bioparticles to achieve the highest sample recovery and good separation. For maximum recovery, separation membrane should have appropriate pore size and molecular weight cut off (MWCO) and a good surface homogeneity without any interactions with biopolymers and bioparticles. The most commonly used membrane has been regenerated cellulose (RC) with a 10^4 MWCO [36]. Hupfeld et al. optimized the operational parameters for liposomes with EgPC and soy-PC, and reported that even RC membranes are prone to adsorption when the sample concentration is less than 0.5 μg [37,38]. However, the adsorption can be overcome by pre-saturation of the RC membrane with sample load of 2 μg or above. For high sample loads, adsorption was minimal, and the recovery was improved. Lang et al. [39] studied the impact of membranes on the separation of negatively charged virus like particles (VLP). Three types of membranes were tested, regenerated cellulose (RC), triacetate cellulose (TC) and polyethersulphone (PES) [Table 1]. Recovery of VLP with an RC membrane was higher than with the other membranes. This could be related to the fact that the negatively charged VLP are electrostatically repelled by the negative charge of RC residues.

In addition to the membrane selection, experimental conditions such as the flow rate, carrier composition and concentration, pH, and sample load found in recent studies are listed in Table 1. The experimental conditions clearly depend on the sample type [36–43]. The common rule for selecting the experimental parameters is that retention time of analyte should neither be too short to avoid the elution in the void peak nor too long to avoid excessive analysis time. Giddings et al. predicted already in 1978 that retention volume (V_r) of an analyte should be higher than $2V^0$. [44]. Nowadays AsFlFFF equipped with field strength programming and miniaturized AsFlFFF provide shorter analysis times.

6. Detection techniques used in asymmetrical flow field-flow fractionation

UV–vis detector is the most commonly used in all the FFF subtechniques, because of its availability, simplicity and low cost. However, the choice of UV–vis is not always straightforward for quantitative work with particles or macromolecules, because some compounds, such as cellulose and its derivatives or sugars, do not at all or only slightly absorb the UV–vis light, or both scattering and absorption contribute to the UV–vis response [38]. The scattered signal is a complicated function of the size and shape of the particles and it increases the detection signal resulting in enhanced concentrations especially for large particles. In flow-assisted methods such as FFF and using a DAD UV/vis detector, Zattoni et al. [45] obtained quantitative results for dispersed (macromolecules or particles) samples. The universal dRI detector plays also an important role in FFF applications, although its sensitivity and stability is not always the best. In addition, flow-through fluorescence detector is an excellent choice for samples that have suitable fluorescence properties [46]. The coupling of MALS detector to AsFlFFF has become more and more popular since it provides the most straightforward results in the determination of the molar masses and sizes of a wide range of biopolymers and bioparticles. With the help of MALS together with UV, the light scattering caused by UV can be corrected. Also nano DLS coupled to AsFlFFF is nowadays quite frequently applied in the measurement of the hydrodynamic radius [47–49].

Mass spectrometry (MS) has already become an important tool in the analysis of biopolymers and bioparticles. Also HFFlFFF, the variant of FlFFF, has been on-line coupled with electrospray ionization/time-of-flight mass spectrometry (ESI/TOFMS) [50]. The system was applied to the analysis and characterization of intact proteins. At the moment the interest in the off-line coupling of conventional or miniaturized AsFlFFF with nanoflow LC–ESI-MS–MS is emerging progressively [11,31,51–54]. The protein fractions collected off-line can be digested followed by peptide analysis carried out by *n*LC–ESI-MS–MS for shotgun analysis.

When other techniques such as LC or isoelectric focusing (IEF) are on-line coupled with AsFlFFF, more proteins can be fractionated. In our recent studies, we used comprehensive two-dimensional AsFlFFF–RPLC for the analysis of proteins from the white part of egg (albumin part without egg yolk) [55]. With AsFlFFF (off-line) four peaks corresponding to proteins with diameters of 4, 5.5–6.0, 7.5–8.0, and 10.0–11.0 nm were identified as lysozyme, ovalbumin, ovotransferrin, and as a dimer of ovotransferrin. With a 10-port interface valve, AsFlFFF fractions were transferred to a reversed phase LC. The RPLC separation was optimized with a gradient program, and the cycle time of 5 min was applied in order to obtain sufficient separation of the FFF fractions. 2D AsFlFFF–RPLC enabled the successful separation of 12 compounds (Fig. 3).

Kim and Moon [56] employed 2D IEF-AsFlFFF. First, the protein standards were separated according to their pIs along an IEF channel located at the head of six AsFlFFF parallel channels. Then the fractionated protein bands were directed to six multilane AsFlFFFF channels for the size-based separation. The study was applied to the 2D fractionation of the human urinary proteome sample under two ampholyte solutions with different pH ranges (pH 3–10 and 3–6). The entire 2D separation was achieved in less than 30 min. The collected protein fractions from 2D IEF-AsFlFFF were digested for peptide analysis and then analyzed by *n*LC–ESI-MS–MS resulting in the identification of 245 urinary proteins.

Table 1
Collection of the optimized parameters recently applied in AsFlFFF for the characterization of biopolymers and bioparticles.

Analyte	Channel, L (cm), w (μm)	Membranes 10^4 MWCO	Cross flow (ml/min)	Focus flow (ml/min)	Load (μg)	Carrier	Detectors	Remarks	Ref
Protein aggregates, and particles	25 cm, 490 μm or, 15 cm, 490 μm	RC	2	1 (4 min)	4–6	PBS	UV–MALS	Recovery high Separation efficiency high	[36]
Liposome: EPC PC LUV, Soy PC LUV	26.5 cm, 250 μm	C	Gradient, 1 to 0.1, in 35min	2 (7 min)	10	10 mM $NaNO_3$	UV–MALS-dRI	Focus flow had a minor effect on separation, instead mass load, cross flow, ionic strength had the major influence on separation	[37,38]
VLP (nicotine vaccine, NicQb)	25 cm, 350 μm	RC TC PES	2	0.2 (5–10 min)	20	20 mM PBS, 150 mM NaCl, pH 7.0	UV–MALS	Recovery of VLP: 96%, with RC, 79% with TC, 30% with PES	[39]
Calsequestrin aggregation	26.5 cm, 350 μm	PES	2	2.2 (5 min)	140	10 mM TRIS, 100–500 mM KCl, 0–10 mM $CaCl_2$, pH 7.2	UV–MALS-dRI	Recovery: 96–111% K^{1+} and Ca^{2+} optimized at 300 mM and 3 mM	[40]
Alginate polysaccharide	27.5 cm, 350μm	RC	0.25	0.2(6.5 min)	100	50 mM NH_4Cl, 50 mM NaCl; or 5 mM NH_4Cl, 5 mM NaCl	MALS-dRI	Recovery:79% (when carrier was 50 mM NH_4Cl, or 50 mM NaCl);recovery:96% (5 mM NH_4Cl, or 5 mM NaCl)	[41]
Influenza virus samples	26.5 cm, 350 μm	RC	grad: 0.4–0 ml/min in 35 min	0.6 (15 min)	na	0.1 M potassium phosphate, pH 7.4	UV–MALS	Focusing time and cross flow optimized	[42]
VLP from Sf9 insect cells	26.5 cm, 350 μm	RC	0.5–1.25	1.5 (6 min)	20	10 mM Tris (pH 8.0), 50 mM NaCl, 10 mM $CaCl_2$	UV–MALS	Cross flow optimized 0.75 ml/min	[43]

Channel flow rate 1 ml/min except for VLP (nicotine vaccine, NicQb) 1.5 ml/min, and for VLP from Sf9 insect cells 0.75 ml/min.
RC, regenerated cellulose; C, cellulose; TC, triacetate cellulose; PES, polyethersulphone.

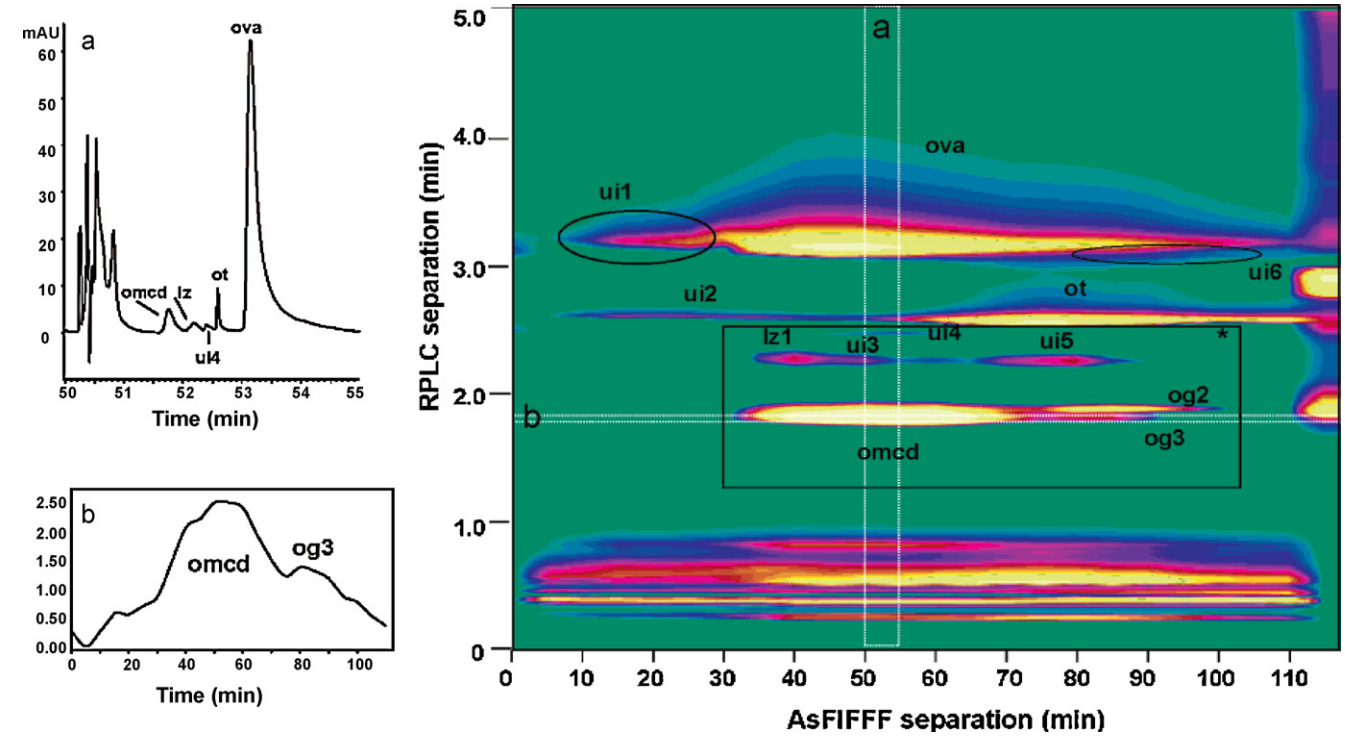

Fig. 3. Fractograms obtained by AsFlFFF (on-line) for crude egg white. Color plot of AsFlFFF–RPLC analysis of egg white sample. The area marked with an asterisk (/) has been zoomed to show the minor components. (a) is a slice of the RPLC separation at retention time 50–55 min showing the separation of compounds with sizes corresponding to 6.1–6.9 nm. (b) Slice of the AsFlFFF separation at RPLC retention time of 2 min, showing the size separation of ovomucoid (omcd) and G3 ovoglobulin (og 3). Flow rates during the elution period were V_{out} 0.08 ml min^{-1} and V_{cout} 2.91 ml min^{-1}. Abbreviations: lz, lysozyme; og 2, G2 ovoglobulin; ot, ovotranferrin; ova, ovalbumin; and ui, unidentified compound. (For interpretation of the references to color in this figure caption, the reader is referred to the web version of the article.)
Reprinted with permission from Ref. [55]. Copyright 2007 American Chemical Society.

7. Asymmetrical flow field-flow fractionation applications to biopolymers

Biopolymers are a class of polymers that are synthesized by living organisms, namely proteins, nucleic acids and polysaccharides [57]. Biopolymers are distinguished according to their chemical structures and functionality. Understanding of their physicochemical behavior and their response to external stimuli is important in order to improve their functionality. Some factors of the external stimuli that affect biopolymer include temperature, electric and magnetic field, solvent, mechanical stress and strain, ionic strength and pH. There are a vast number of established methods that help to examine the physicochemical behavior of biopolymers [58]. At the moment, size exclusion chromatography (SEC) is the most commonly used technique for the characterization of biopolymers [59]. This high throughput technique is sensitive, reproducible, and relatively easy to use and validate. However, SEC has also some limitations. It separates aggregates over a limited size range and has a poor resolution for larger soluble aggregates, which may be eluted out at the void volume. Analytical ultracentrifugation is an alternative to SEC for analyzing biopolymers with a wide range of hydrodynamic radius to obtain information about their size and shape, and the thermodynamic information related to the molar mass, conformation, association constants, and stoichiometry of reactants [60–62]. Methods like capillary electrophoresis and gel electrophoresis are also frequently used for the fractionation of biopolymers and bioparticles in accordance with their size [63–65]. AsFlFFF is either alternative or complementary technique to SEC depending on the application. It is a gentle method allowing the full range characterization of biopolymers starting from proteins to large polysaccharides, either in native or aggregated (denatured) forms.

7.1. Proteins

As early as in 1976 FlFFF was considered to be a versatile method in the characterization of biopolymers [12]. Since then, separation speed, and separation efficiencies have been greatly improved. The use of MALS detector with AsFlFFF/FlFFF provides accurate size, shape and molar mass information of biopolymers including proteins and protein aggregates, without the need of calibration with standards of known molar masses [66,67].

Another benefit of AsFlFFF–MALS is that the technique allows the separation of monomer proteins from aggregates in one run, and the determination of the sizes and the molar masses of each fraction at the same time. The characterization of protein aggregation is important especially in the case of therapeutic proteins. Cao et al. [36] and Gabrielson et al. [61] quantified the recombinant humanized monoclonal antibody aggregate levels by using SEC, AsFlFFF and analytical ultracentrifugation (AUC). AsFlFFF and AUC provided more accurate particle sizes and molar masses on soluble aggregates than SEC, and both AsFlFFFF and AUC techniques proved to be reliable, powerful and versatile for the measurement of protein aggregates in pharmaceutical industries and biotechnology applications.

Often external stimuli, such as temperature, pH or ionic strength, enable proteins to form partially unfolded monomers or completely denatured unfolded aggregates [68]. In some cases, self-association of polypeptides can lead to aggregation as an abnormal protein deposit, such as amyloid fibrils and prion infections. These are insoluble fibrillar depositions in the brain signaling to neurodegenerative diseases. Amyloid β-protein ($A\beta_{1-42}$) monomers associate into soluble intermediates, such as oligomers and then into insoluble fibrils. The time dependent amyloid $A\beta_{1-42}$ aggregate formation was monitored by AsFlFFF–MALS, and the data indicated that the dynamic aggregation processes caused changes in the molar mass and size of the aggregates [69]. AsFlFFF connected to MALS and DLS was implemented to study the abnormal aggregation of prion, and the relationship between the size and the infectivity of Prion Protease-Resistant (PrPres) [70]. According to AsFlFFF results, the molar mass of the PrPres aggregate was 6×10^4–1×10^7 g mol^{-1}, the rms size (R_g) 10–250 nm, and the rh size 5–200 nm. From the earlier fractions, the ratio rms/rh was ~0.9, an indication of discoidal shape of the aggregates, where as for the late fractions, rms/rh was >1, a more extended shape for such kind of fibril. The AsFlFFF–MALS–DLS results were comparable with transmission electron microscopy images. The infectivity of PrPres was highest for particles of 17–27 nm (3–6×10^5 g mol^{-1}), whereas the activity was substantially lower for large fibrils. AsFlFFF–MALS was also applied to the determination of the particle sizes of the bacterial Inclusion Bodies (IBs) that contain amyloid-like aggregates [71]. The data indicated that dynamic aggregation processes were involved in the molar mass and size of the aggregates. Additional studies on prion aggregates and IBs can be found elsewhere [7,11]. Glucagon, a 29-residue peptide hormone is used as a therapeutic agent, including the emergency treatment of hypoglycemia. *In vitro* it has a tendency to aggregate and form fibrils and gels. The physical instability of glucagon causes problems in formulation, and in the delivery of its pharmaceutical product. Hoppe et al. [67] investigated the initial aggregation formation, i.e. the seed nuclei of glucagon in acidic and alkaline media by AsFlFFF–MALS, SLS and DLS. DLS indicated bimodal distributions with 1 nm and 100 nm of radius for the monomer and aggregate, respectively. The aggregate was removed by filtration from acidic but not from alkaline solutions. After the sample filtration AsFlFFF–MALS allowed the separation of monomers from aggregates. It was possible to quantify both bimodal distributions, and molar masses were 3.7×10^3 g mol^{-1} for the monomer and 1.9×10^6 g mol^{-1} for the aggregate from both filtered and non-filtered samples (Fig. 4).

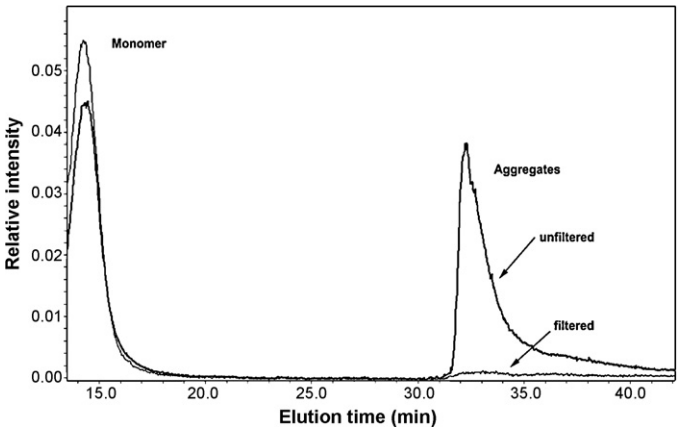

Fig. 4. AsFlFFF–MALS fractograms from glucagon monomers and aggregates, filtered and non-filtered samples. Carrier 0.1 N HCl.
Reprinted with permission from Ref. [67]. Copyright 2008 BioMed Central Ltd.

The pH and the ionic strength of carrier solution have been found to alter the charge distribution of amino acid side chains of proteins which either decrease or increase the protein–protein interactions. Song et al. [72] noticed when they clarified the effect of carrier composition (ionic strength and pH) on the retention of various proteins that the retention and size of proteins increased with the increasing ionic strength.

The Calsequestrin (CSQ) with native molar mass of 4.53×10^4 g mol^{-1} is known to sequester and release calcium accumulated in the sarcoplasmic reticulum of muscle cells during relaxation. The experimental studies carried out by Shadle et al. [40] agreed with the theoretical calculations about the importance of Ca^{2+} in the formation of different protein structures. First dimers

were seen with molar mass of 9.0×10^4 g mol^{-1}, then tetramers with molar mass of 1.8×10^6 g mol^{-1} followed by higher order aggregates. The effect of K^{1+} was slightly different, because the dimer was dominant over monomer, tetramer, and other aggregate species.

The role of Mg was also clarified on in the aggregation of a therapeutic IgG (antibody A) with nominal molar mass of 1.5×10^5 g mol^{-1} [73]. The protein was dissolved into two buffer solutions, one containing 50 mM $MgCl_2$ in 0.1% acetic acid, and the second one, 10 mM sodium phosphate buffer at pH 7.1. The protein solutions were characterized by using DLS, AsFlFFF–MALS, fluorescence microscopy, circular dichroism, and fluorescence lifetime spectroscopy. AsFlFFF–MALS showed in 0.1% acetic acid containing 50 mM $MgCl_2$ 88% monomer (1.6×10^5 g mol^{-1}), 2% dimer, and 10% of higher molar mass aggregates (>10^6 g mol^{-1}). In phosphate buffer solution without Mg^{2+} ions, high molar mass aggregates were not seen, because the aggregates formed in phosphate buffer were probably disrupted during FFF analysis due to weak interactions. The combination of several analytical techniques collectively allowed a reliable assessment of protein self-association and aggregation phenomena. Samontha et al. [74] used AsFlFFF and sedimentation FFF (SdFFF) under such conditions that led to hen egg white protein aggregation. At pH > 5 with protein concentration of 2%, and ~25 mM $ZnCl_2$, AsFlFFF and SdFFF could be efficiently utilized to control the aggregate size of hen egg white protein.

Recently, AsFlFFF–UV–MALS was applied to clarify the effect of heat on bovine serum albumin (BSA) [75]. In addition to the different heating rates, different concentrations of NaCl and SDS, and different time of incubation were tested. Under non-heat stress, the proteins produced monomers and dimers, whereas during the heat stress, the third peak at about 63 °C (onset temperature) appeared, indicating that the proteins were denatured and started to form aggregates. When the temperature increased beyond the onset temperature, the molar mass and the particle size of the aggregates further increased. The particle sizes of the aggregates were dependent on the degree of heating, the time of incubation, concentration of the proteins and the concentration of salt. Because thermal induction with SDS produced only one monomer peak, the addition of SDS at higher temperatures stabilized protein samples, whereas sodium chloride resulted in increased aggregation. The hydrophobic alkyl chain of SDS associated with the hydrophobic parts of BSA, and the hydrophilic sulphate group of SDS was bound electrostatically to the positively charged amino acid groups of proteins. In both cases the proteins remained negatively charged and aggregates were not formed. The results agreed with those obtained by Samontha et al. [74].

Thermally induced aggregation and conformational change of immunoglobulin (IgG) was clarified by high-pressure size exclusion chromatography (HP-SEC) and AsFlFFF [46]. Both techniques were connected to UV, MALS and to on-line fluorescent dye detector. The dye was added either to the carrier or to the sample. The fluorescence detector was more sensitive than UV or MALS detectors for both IgG monomer and the thermally induced aggregates. HP-SEC provided a better separation for monomers and dimers, whereas AsFlFFF enabled the analysis of larger aggregates of heat-induced IgG. After heating, the fluorescence was increased due to the formation of aggregated IgG and the conformational change of the protein.

7.2. Nucleic acids

Research related to DNA delivery into cells is one of the central issues in molecular biology. DNA delivery is also a critical process in *in vivo* applications such as gene therapy, vaccination, and drug development. Self-assembled cationic lipid–DNA complexes are promising method capable to carry DNA across the cell membranes and applied in gene therapy. The size of DNA and RNA is commonly measured by gel electrophoresis and detected by ethidium bromide, or Coomassie Brilliant Blue. Chromatographic methods and FFF are also applied to the characterization of DNA and DNA complexes. Among the FFF methods, FlFFF/AsFlFFF are widely used to characterize nucleic acids, just like in the work of Lee et al. where heterogeneous mixtures containing lipids, DNA, liposomes, and lipid–DNA complexes were characterized by FlFFF-MALS [76]. The measurements showed that different lipid/DNA-ratios resulted in different size profiles. FlFFF–MALS paved a detailed examination of subtle changes in the physical properties of nonviral vectors and provided a basis for the definition of structure–activity relations for lipid–DNA complexes as novel class of pharmaceutical agents.

Ma et al. studied complex formation between DNA and chitosan cationic polysaccharides [49]. The authors used on-line AsFlFFF–UV/vis–MALS–DLS for the measurement of the size and size distribution of the complexes together with the content of unbound polycation (chitosan). To facilitate the UV/vis detection, the chitosans were labeled with rhodamine B. AsFlFFF analysis revealed that 73% rhodamine labeled chitosan remained free in solution during the formation of complexes, and that the size of the DNA/chitosan complexes ranged from 20 to 160 nm in hydrodynamic radius. It was concluded that the AsFlFFF combined with DLS allowed the characterization of small particles at low concentration that were not detected by conventional batch-mode DLS.

7.3. Polysaccharides

The molar mass and molar mass distributions essentially influence the functionality of polysaccharides in a variety of applications. However, these substances are heterogeneous and polydisperse [77]. Some are linear and others branched, some neutral, and others charged. They can also self-associate and have such a conformation in solution that is difficult to precisely define, e.g. starch, or cellulose, whose polydispersity is large, and where large-sized aggregates up to several hundred nm may occur [78].

AsFlFFF with multiple detection is a powerful tool for obtaining data of hydrodynamic radius, radius of gyration, molar mass, polymer conformation, and branching degree, all properties important for polysaccharides with complex structures. Comprehensive reviews on the applicability of AsFlFFF to the characterization of linear and branched starches, modified cellulose, polysaccharide derivatives, glycoproteins (mucin, gum Arabic) are found in the literature [7,10,11]. In AsFlFFF analysis, the correct experimental conditions were established for the retention and characterization of alginate polysaccharides [41]. Under these optimal conditions, alginate molecular characteristics, M_W 1.8×10^5 g mol^{-1} and R_{gw} 50 nm were obtained by AsFlFFF–MALS-dRI. Storz et al. used AsFlFFF–MALS as a complementary technique to SEC in studies of viscous alginates [79]. The results achieved with both these techniques agreed well for the analysis of low molar masses (<2.1×10^5 g mol^{-1}). However, getting molecular mass information for ultra-high viscous alginates with 2.1×10^5 g mol^{-1} or above was possible only with AsFlFFF, especially when alginates were modified by covalent fixation of poly(ε-caprolactone) pendant chains onto the polysaccharide backbone via ester links [80]. Pitkänen et al. analyzed aggregation behavior from arabinoxylan polysaccharides in aqueous solution and compared results obtained by using AsFlFFF–MALS with those obtained with HPSEC connected to dual angle light scattering, viscometer and dRI detectors. [81]. The molar masses < 2.4×10^5 g mol^{-1} and R_g < 42 nm achieved with these two techniques agreed well with each other, but three-fold bigger aggregates were seen only by AsFlFFF–MALS.

Physically and chemically modified starches have been studied for various purposes. Depending on the type of derivatization,

degradation of the original starch structure may occur, resulting in a change of molar mass and R_g. It is therefore necessary to know the molar mass and the possible conformation of the derivatives. AsFlFFF–MALS showed a significant decrease of both molar mass and R_g in studies of mechanical degradations caused by high-pressure homogenization and thermo-mechanical extrusion [82–84]. High shear rate may break down the hyperbranched polymers and reduce the fractal aggregates. In the chemical degradation studies of starch AsFlFFF–MALS provided the reduced molar mass and R_g values from cationic starch derivatives. Tailing was seen in the elution profile due to attractive interaction between cationic starch molecules and the channel membrane, and repulsion among cationic starch molecules.

Rolland-Sabaté et al. studied the nature of amylopectins branches from different botanical sources and glycogen from rabbit liver [85,86]. Starches were dissolved in DMSO, and then resolubilized using microwave heating under pressure. Glycogen sample was solubilized in water. AFFFF enabled a good fractionation for amylopectins and glycogen leading to detailed macromolecular characteristics (Fig. 5Aand B). Amylopectin M_w, R_g, and the hydrodynamic coefficient ν_G (the slope of the log–log plot of R_{Gi} versus M_i) were within the ranges of 1.0–4.8 × 10^8 g mol^{-1}, 110–267 nm, 0.37–0.49, respectively. The data achieved for hyperbranched polymers followed an ABC theory model. For rabbit liver glycogen M_w and R_g were 1.39 × 10^7 g mol^{-1} and 28.7 nm, respectively. The relationship between R_g (obtained from the MALS data) and the molar mass (obtained from the ratio of the LS scattering and the RI signals) over the size distributions provided the information on the density and branching of the different samples. Waxy maize starch was found to have the highest degree of branching, followed by normal maize amylopectin, cassava amylopectin, waxy rice starch and smooth pea amylopectin, waxy barley starch, and finally amylose free potato starch. High mass recoveries were achieved (81.7–100.0%).

Souguir et al. introduced unique characteristics on ampholytic and amphiphilic pullulan derivatives that improve functional properties of the original pullulans depending on environmental conditions (pH, temperature and salinity). The physicochemical characterization determined by AsFlFFF–MALS-QELS [87] revealed the modified derivative of pullulans to have polyelectrolyte-like behavior. In pure water at the isoelectric pH, attraction between positive and negative charges led to relatively tight coiling of the polymer. Far above and below the isoelectric pH, the polymers had highly expanded structure. These ampholytic polysaccharides have opened a new avenue for adjustable and flexible systems with great applicability, especially in the field of drug controlled release.

AsFlFFF–MALS was successfully applied to various commercial chitosan types that are modified from chitin polysaccharides that have applications in pharmaceutics, e.g. as excipient or drug carrier. Chitosan embraces a series of polymers that vary in molecular weight from ∼10^4 to ∼10^6 g mol^{-1}. Mao et al. [88] investigated the feasibility of AsFlFFF–MALS to measure the molar mass of chitosans, compared with the results obtained by intrinsic viscosity and SEC methods. The polymers were 2.5–10 × 10^4 g mol^{-1}. Similar values were achieved by the three methods, although they were based on measurements of different parameters. The data confirmed that AsFlFFF–MALS is a powerful tool for the characterization of chitosans. Augsten and Mäder [89] extended the range of molar mass analysis to ∼4 × 10^5 g mol^{-1}. Most of the measured samples followed molar mass distributions of monomodal logarithmic Gaussian type. The conformational parameters were verified to be molar mass dependent, ranging from open structures molecules to theta coil conditions or an even more compact conformation.

Hyaluronan, also known as hyaluronate or hyaluronic acid (HA) is biocompatible and biodegradable polymer with possible applications in drug delivery, ophthalmic surgery, wound healing, and tissue engineering. A series of papers have been published in which AsFlFFFF–MALS was applied to study the degradation of ultrahigh-molecular weight hyaluronate under the influence of thermal stress [90], ultrasonic, enzymatic or pH [91]. Electron irradiation effect was applied to study scleroglucan degradation, because of its resistance to hydrolysis, temperature and electrolytes [92], and via AsFlFFF the presence of low and high molar mass fractions could be proved.

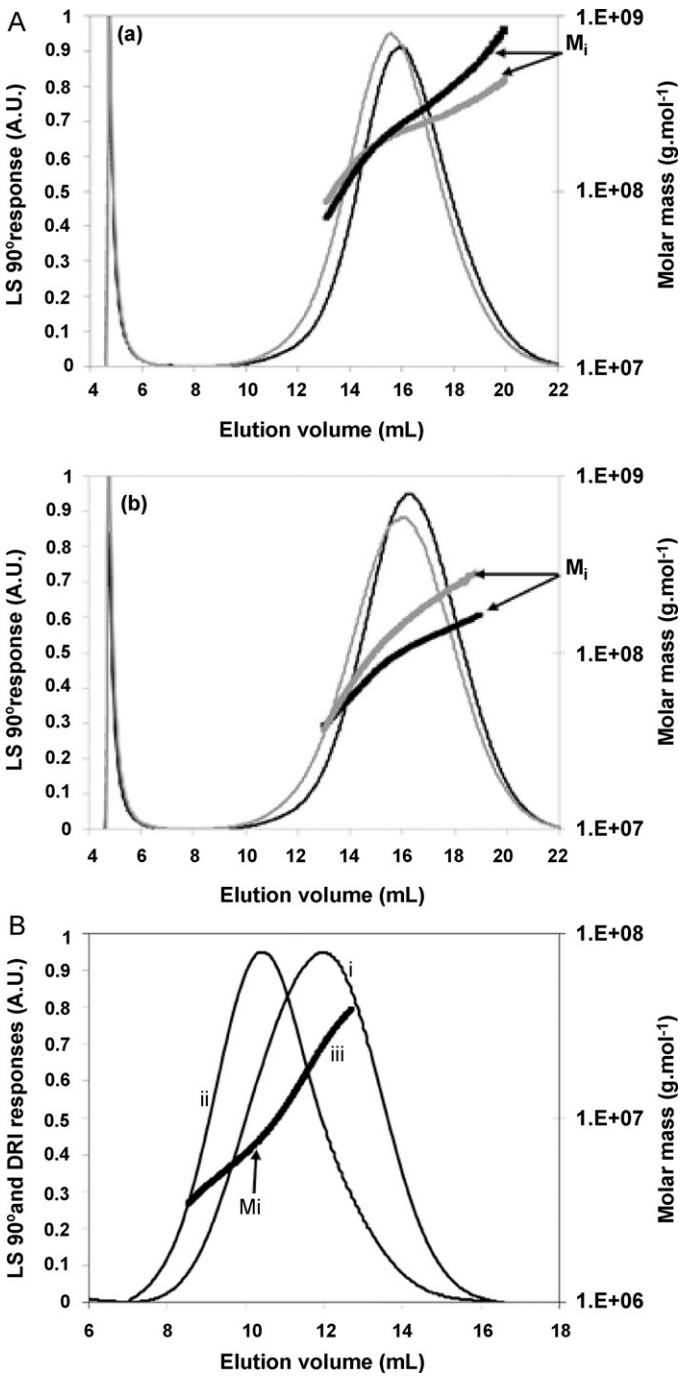

Fig. 5. (A) Elugrams (LS 90° responses) of amylopectins and their molar masses versus the elution volume (V_i): (a) waxy wheat starch (black) and waxy rice starch (gray); (b) amylose free potato starch (black) and cassava amylopectin (gray). The thin lines represent the LS 90° responses, and the thick lines the molar masses. (B) Elugrams (LS 90° (i) and DRI (ii) responses) of rabbit liver glycogen and its molar masses (iii) versus the elution volume (thick line).
Reprinted with permission from Ref. [85]. Copyright 2007 American Chemical Society.

8. Asymmetrical flow field-flow fractionation applications to bioparticles

Biological cells and microorganisms produce proteins and other products known as bioparticles. The products are either excreted into the medium or accumulated inside the cells. Separation and characterization of cells, microorganisms and their products is essential to design products of biotechnological, biomedical and pharmaceutical interests. Bioparticles have a large variation in size, shape and composition. Determination of these properties is therefore essential for optimization of the processing and design. Particle sizing methods are widely available. Examples are light microscopy, electron microscopy, capillary zone electrophoresis, sedimentation analysis, the electric sensing zone method, and field-flow fractionation. Each of these methods has its own restrictions and applicability depending on the specific particle mixture that needs to be analyzed. This review discusses application of AsFlFFF. The use of other methods has been extensively treated in literature. Due to the combination of both normal and steric separation modes, AsFlFFF can be applied to the analysis of wide range of bioparticles, including proteins, nucleic acids, protein complexes, viruses, virus like particles, lipoproteins and liposomes, microbes, cellular organs and animal cells. The application of AsFlFFF to proteins and nucleic acids is already discussed in Sections 7.1 and 7.2.

8.1. Virus and virus-like particles

Viruses are among the first bioparticles studied by FlFFF/AsFlFFF [93]. Depending on size differences, a mixture of viruses and BSA as a marker were separated by flow FFF. Virus-like particles (VLPs) are an important class of bioparticles composed of self-assembling viral proteins excluding their genetic materials [94]. These particles are candidates for vaccines, gene delivery vehicle, and drug therapies [95]. The particles consist of an inactivated virus or a surface antigen of a virus that is produced by a genetically modified microorganism. To recover the VLPs, the cells have to be disrupted, thus creating a mixture of cell debris and VLPs. It is clear that the production of these VLP bioparticles gives rise to a particle–particle separation from the rest of cell debris. A reliable advanced analytical tool is therefore needed to control the process and to assure the quality of the final product. The gentle separation mechanism of AsFlFFF, by which the structure and conformation of analytes is preserved, makes it a very valuable technique for the precise characterization of VLPs.

The composition of VLP is classified by AsFlFFF into different fractions, i.e. VLP fragments, monomers, dimers, oligomers and aggregates [39,96]. The presence of these fractions was confirmed by TEM analysis. AsFlFFF–MALS accurately quantified and determined the molar masses, 3.27×10^6, 6.27×10^6 and 9.80×10^6 g mol^{-1} for the monomer, dimer and trimer, respectively (Fig. 6). The shoulder on the left side of the main peak comprises VLP oligomers or aggregates in the range of 10^7 or 10^8 g mol^{-1}. Compared to DLS and SEC, AsFlFFF exceeds the capabilities of these commonly applied methods with regard to the analysis of the physical properties of VLPs. The results demonstrated the high potential applicability of AsFlFFF for the investigation of VLP in pharmaceutical product formulations. Further, AsFlFFF–MALS was used to monitor the stability VLP with a model of a nicotine vaccine (NicQb). The data showed that, the stability of NicQb vaccines in solutions was strongly influenced by solution conditions like pH, ionic strength, osmolarity, and the presence of excipients, such as surfactants, polyols, sugars, and salts on the stability in liquid formulations. The stability was confirmed at pH 6.2

Wei et al. studied influenza virions (avian influenza) for vaccine development. The vaccines were produced from the allantoic fluid of developing chicken embryo. The process of viral replication

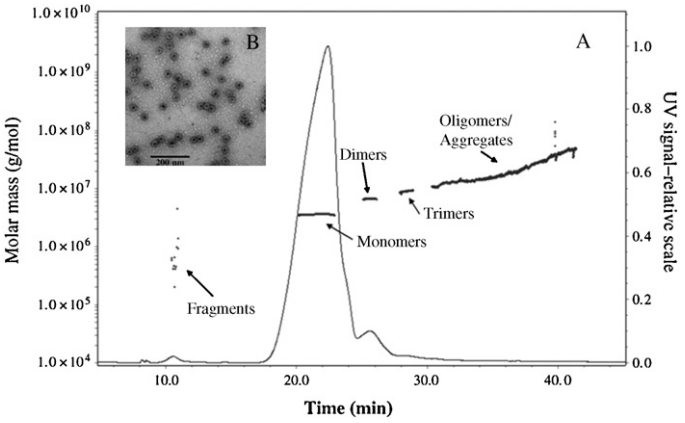

Fig. 6. Fractionation of VLP-NicQb AsFlFFF–MALS, UV signal (continuous line) and molecular weight (dots) calculated from respective UV and multiangle light scattering (MALS) signal (A). Transmission electron microscopy (TEM) picture of NicQb (B).
Reproduced from Lang et al. [96]. Adapted by permission from Informa Healthcare: [Drug Dev. Ind. Pharm.] (35 (2009) 83), copyright (2009).

that produced a heterogeneous mixture of infectious and non-infectious viral particles with varying states of aggregation was analyzed by AsFlFFF–MALS, SEC-MALS, TEM, and AFM [42]. With optimized focusing time and cross flow, AsFlFFF–MALS proved to be an effective tool for measuring total particle counts and the number-weighted size distribution of influenza virions. The correlation between the various methods for determining total particle counts, infectivity and size distribution was attained. Chuan et al. also described AsFlFFF a reliable method for VLP analysis by comparing it with DLS and TEM [43]. The authors optimized AsFlFFFF that did not cause significant aggregation, and provided an accurate size and distribution information that was not possible with TEM and DLS. With the optimized AsFlFFFF, the batch consistency for new vaccine products was monitored and unique information on the whole population of the particles within a sample was provided.

AsFlFFF was employed for the development of a gene-delivery vehicle based on VLPs derived from the human polyoma JC virus [97]. The gene delivery vehicle was created by re-assembling the recombinant protein VP1 pentamers in the presence of the desired DNA. The newly formed VLPs encapsulated with the new DNA showed delivering the gene of interest to target cells where it was translated into protein. With AsFlFFF combined with diode array, fluorescence, MALS, DLS, and dRI detectors, it was possible to characterize the intermediates and final drug products. From a single analysis, the molar mass, root mean square radius and hydrodynamic radius, composition, and purity of the samples were determined.

In the work of Lipin et al. murine polyomavirus (MPV) was used as a representative sample of soluble protein aggregate i.e. a precursor of self-assembled VLPs [98]. AsFlFFF–MALS and DLS were used to monitor whether aggregation was able to prevent enzymatic cleavage of tagged glutathione-*S*-transferase (GST) purified viral protein (VP1). Both methods showed the protein existed as soluble aggregate that can be filtered out through a 0.22 μm filter, which implied that aggregation did not appear to affect the quaternary structures of the VP1 pentamers. Further, AsFlFFF–MALS quantified the molar mass distribution, and the results were 60 kDa to 20 MDa from the protein aggregates. AsFlFFF–MALS proved to be an ideal analytical method to determine the size distribution of the GST-tagged VP1 soluble aggregates. The authors also successfully utilized AsFlFFF- MALS to identify structural conformation in murine polyomavirus virus-like particles (MPV VLPs), as a result of encapsulation with genomic DNA and non-viral protein. Encapsu-

lation of non-viral protein into MPV VLPs also appeared to prevent DNA encapsidation, without modification of the VP1 sequence and while maintaining VLP assembly within the nucleus. From the work of Pease et al., VLPs derived from the non-enveloped murine polyomavirus (MPV) were characterized by AsFlFFF–MALS, electrospray differential mobility analyzer (ES-DMA) and TEM. These three techniques detected size differences due to subtle changes in the production processes. The authors demonstrated that ES-DMA and AsFlFFF–MALS were able to quantify VLP size distributions with greater rapidity and statistical significance than TEM, providing useful technologies for product development and process analytics [99].

8.2. Lipoproteins and liposomes

Plasma lipoproteins are lipid protein complex bioparticles that are responsible for transport lipids, cholesterol and triglycerides in blood. These bioparticles are divided into five major subclasses on the basis of the density at which they float during ultracentrifugation. Lipoprotein subclasses are further divided according to particle size, electrical charge and apolipoprotein and lipid contents.

AsFlFFF has been shown to be a powerful, sensitive analytical tool in the study of lipid transfer mechanisms. Setälä et al. used AsFlFFF to follow the transfer mechanisms of phospholipids and phospholipid transfer proteins (PLTP) between small unilamellar lipid vesicles (SUV) and HDL [100]. Radio-labeled SUV, PLTP and HDL were allowed to exchange lipids, and after the reaction, the SUVs and HDL were separated by AsFlFFF. Rambaldi et al. studied the feasibility of FlFFF–MALS as a method for size and shape characterization of lipoproteins [101]. Their data was in accordance to discoidal conformation. Variations in concentration, composition, and particle sizes of lipoprotein are factors in the development of atherosclerosis, the leading cause of heart failure. AsFlFFF was hyphenated with on-line enzymatic detection, and was able to quantify cholesterol and triglycerides associated to each fractionated lipoprotein classes [102,103]. Results obtained from healthy serum donors agreed well to values obtained by a clinical laboratory. Results achieved on serum samples from a healthy donor and from a patient affected by sepsis showed significant differences in the profiles of cholesterol and triglycerides associated with the fractionated lipoproteins. In the work of Witos et al. mono and disaccharide sugars (20% m/m) were applied to suppress the particle sizes of lipoproteins [104]. The authors used capillary electrophoresis, dynamic light scattering and AsFlFFF to evaluate the effect of sugars on lipoprotein particle size suppression. According to DLS and AsFlFFF results, the particle size of HDL was reduced by 30% from its native size, whereas the particle size LDL reduced only by 1.7-4.3%. Sugars treated lipoproteins were successfully separated using capillary electrophoresis with uncoated capillaries.

Liposomes are self-assembled colloidal dispersions that mimic cell membranes. An attractive feature of liposomes is that they are biocompatible for drug delivery in various pharmaceutical and biotechnological applications [105]. Physical properties of the liposomes can be readily modified. Size, charge, rigidity, and surface properties can be altered by using different liposome preparation methods and lipid compositions [106], the concentration of the molecules, and different surrounding properties, such as temperature, solvent composition and ionic strength. The size of the liposome in dispersions varies from 20 nm for small unilamer vesicles to about 200 μm for giant vesicles. Particle size and size distribution are characteristic factors for liposome-based drug delivery systems that determine colloidal stability, encapsulation efficacy, bioavailability, and targeting ability. There are several analytical techniques including AsFlFFF useful for the determination of aggregated or non-aggregated liposome sizes. The retention behavior of liposomes during the liposome preparation was examined by varying ionic strength and pH of carrier solutions, sample overload effect, membrane type, concentration, flow rate and osmotic pressure [37,38,107]. MALS–UV-dRI detectors allowed successful studies on the size of plain liposomes, actin containing liposomes, and encapsulated liposomes with hemoglobin [108]. From the MALS data it was concluded that empty liposomes and liposomes encapsulated hemoglobin (LEHb) are spherical, while actin modified LEHb have a thin-disk shape. AsFlFFF has been also used to characterize the liposome sizes in the development of new stabilized particle/polymer/protein-covered liposomes, such as liposome encapsulating hemoglobin [108], and that of polyethylene glycol–lipid aggregates containing various types of polyethylene glycol-functionalized lipids [109].

Jores et al. introduced solid lipid nanoparticles (SLN) and oil loaded solid lipid nanoparticles (also named nanostructured lipid carriers, NLC) as novel carrier systems for cosmetic active ingredients and pharmaceutical drugs [110]. The authors used AsFlFFF–MALS combined with photon correlation spectroscopy (PCS), laser diffraction (LD), and cryo transmission electron microscopy (cryo TEM) to characterize the physical behavior of SLNs and NLCs [110]. The results obtained with PCS indicated that SLN and NLC differ from a nanoemulsion with respect to Brownian motion due to asymmetric particle shapes. Non-spherical particles, in the case of SLN and NLC, lead to higher polydispersity indices compared to the nanoemulsion. In AsFlFFF the nanodroplets elute much quicker than SLN-and NLC-platelets although their photon correlation spectroscopy and laser diffraction data show similar particle sizes (Fig. 7). In cryo transmission electron microscopy platelet (for SLN), oil loaded platelet ("nanospoons"; for NLC) and droplet (for nanoemulsion) structures were observed. In contrast to literature reports, the investigated SLN appeared as thin platelets. NLC was found to be as lipid platelets with oil spots sticking on the surface.

8.3. Micron and submicron sized bioparticles

Cells and sub cellular bioparticles ranging from 0.5 to 50 μm in size are considered to act as key players in the solution of human diseases in several biological fields such as hematology, microorganisms, biotechnology, molecular biology, neurology and cancer research. Cell handling requires high specific cell manipulation techniques with possibility for the separation and isolation [111]. Barman et al. [112] used FlFFF and separated red blood cells from human, equine, canine, feline, and bovine. The size based separation achieved by AsFlFFF/FlFFF can help to collect purified fractions for further culture of individual properties of cells, and diagnosis of abnormalities. Saenton et al. [113] evaluated the potential of steric/hyperlayer SdFlFFF, ElFFF and FlFFF for the separation of different bacteria types. Although SdFFF gave higher selectivity, all the FFF subtechniques separated various strains of bacteria and differentiated live bacteria from dead ones. The data indicated that FFF techniques are good analytical techniques for cellular and microbial separations [114]. AsFlFFF was applied to characterize biosurfactants extracted from bacteria that can be found in soil contaminated by an oil spill [115]. From the retention data, d_H and molar mass of the biosurfactant was 49 nm and $2.3 \times 105\ g\ mol^{-1}$ when extracted with n-hexane, and 39 nm and $1.13 \times 105\ g\ mol^{-1}$ when extracted with the 2:1 mixture of chloroform/MeOH. Furthermore, FlFFF was on-line coupled with ICP-MS for studies on uranium bound to bacteria as a function of pH [116]. At pH ~ 5, binding U to bacteria was higher due to complexation of UO_2^{2+} with negatively charged carboxyl groups at the bacteria surface. As the pH was increased, uranium bound to the cell surface decreased, and the complex was not formed. Uranium carbonate and hydroxide passed through

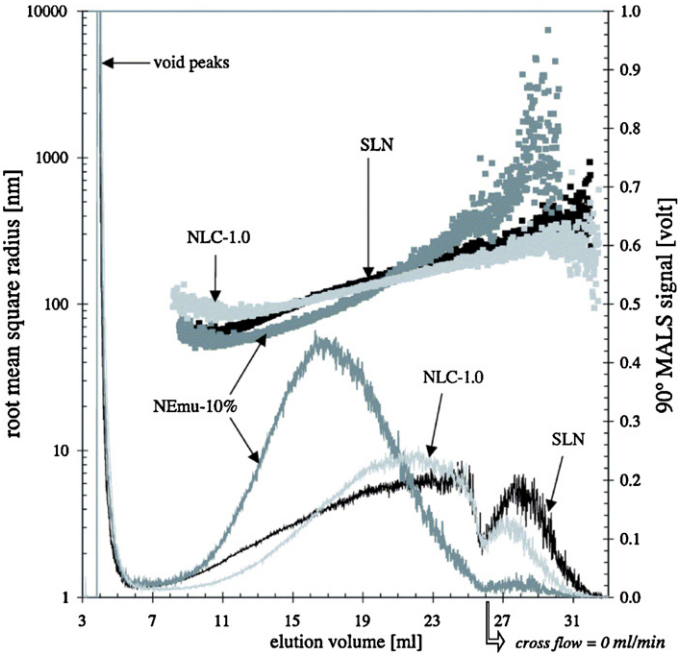

Formulation	Z-average radius [nm] (elution by FFF and subsequent LS measurements of eluates gained in between 8th and 26th minute)	Z-average radius [nm] (elution by FFF and subsequent LS measurements of eluates gained in between 8th and 32th minute)
SLN	185 +/– 4	300 +/– 9
NLC-1.0	160 +/– 3	198 +/– 5
NEmu-10%	273 +/– 9	723 +/– 18

Fig. 7. Elution behavior of lipid nanodispersions by AsFlFFF, subsequently detected by LS (top curves: root mean square radii; bottom curves: intensities of scattered light). Table at the bottom: *z*-average particle sizes of the nanodispersions obtained from the upper graphic.
Reprinted with permission from Ref. [110]. Copyright 2004 Elsevier.

the FFF membrane. AsFlFFF was also used to fractionate micron sized bioparticles and utilised as pre-analytical technique for the characterization of size-dependent proteome patterns [31,33,52]. Additional studies on the applicability of AsFlFFF in proteomics can be found elsewhere [11,53]. Recently, Kang et al. fractionated membrane proteins from whole cell lysates of prostatic cancer cell [117]. The authors compared results with those achieved with conventional AUC method. Eluted lysates from AsFlFFF runs were collected into two fractions. The fractions and AUC were tryptically digested, and the resulting purified peptide mixtures were analyzed by two-dimensional cation exchange-reversed phase liquid chromatography–electrospray ionization-tandem mass spectrometry (2D-SCX-RPLC–ESI-MS–MS). Because the number of protein membranes identified by AsFlFFF and AUC were 172 and 127 respectively, it was concluded that AsFlFFF as a soft preparative method was more suitable than AUC for the isolation of target membranes from cell lysates and for the minimizing the loss of subcellular vesicles.

9. Conclusions

The fundamental principle underlying classical application of AsFlFFF to size based analysis and size based separation (1 nm–1 μm in diameter) is that λ depends solely on the balance of diffusion coefficient and the applied field. The applied field causes the particles to move through the flow profile in a flowing liquid. This creates a differentiation of the particle velocities in the separation device that is the basis for their separation. When the particle size is large enough (>1 μm), separation is feasible on the basis of the lift force. Due to the combination of both normal and steric separation modes, AsFlFFF applications *span a* wide range of biopolymers and bioparticles, including proteins, nucleic acids, polysaccharides, viruses, virus like particles, lipoproteins, liposomes, microbes, cellular organs and animal cells. This review describes different advances and approaches taken for the separation and characterization of biopolymers and bioparticles by AsFlFFF. Frit-inlet-Frit-outlet configuration, focus-flow and slot outlet technologies, or possibilities of using miniaturized AsFlFFF channels have been developed to facilitate its use for biopolymer and bioparticle analysis. Upon down scaling the separation channel geometry to miniaturized scale, it is possible to achieve retention profiles within shorter time periods, with smaller sample amounts, with lower mobile phase consumption, and it is found suitable for coupling to *n*LC–ESI-MS–MS.

Coupling with other techniques such as MALS, DLS, fluorescence and ICP-MS, which provide information about improved level of detection, and the use of highly selective detectors, has widened the applicability of AsFlFFF to several fields including food, pharmaceutical and biotechnology. In food and agro industry analysis AsFlFFF is applied to study protein aggregation during food processing, and characterization of polysaccharides such as physical and chemical modified starches which are difficult to characterize. For these macromolecules detailed data regarding size and conformation can be obtained with AsFlFFF–MALS-dRI. These results can, in turn, be related to thickening and emulsification properties of polysaccharides. In pharmaceutical, biotechnology, and biomedical applications, AsFlFFF is used to separate monomer from aggregates therapeutic proteins, to quantify antibody aggregates, and to determine the size distribution of bioparticles, drug carriers, biopolymers and bioparticles.

Many factors, such as temperature, solvent, mechanical stress, ionic strength and pH, clearly play an important role in physical and chemical characteristics of biopolymers and bioparticles. The effect of temperature induced aggregation and conformational change of BSA and immunoglobulin proteins. pH is seen to affect functional properties of pullulan derivatives. Ionic strengths with Ca^{2+} and Mg^{2+} induced aggregation of Calsequestrin and therapeutic IgG. The influence of mechanical, thermal, enzymatic, pH and irradiator caused degradation of ultrahigh-molar masses of amylopectins, hyaluronates, or scleroglucans.

AsFlFFF is evidently a complementary or even alternative technique to SEC for the analysis of ultra-high-molecular-mass biopolymers, protein aggregates and cells. In the case of IgG protein HP-SEC provided a better separation for monomers and dimers, whereas AsFlFFF enabled the analysis of larger aggregates. In the analysis of polysaccharides both techniques gave similar results when the molar mass was $<2.5 \times 10^5$ g mol^{-1}, whereas AsFlFFF was better for the analysis of ultra-high-masses.

Further optimization of the operational parameters in miniaturized AsFlFFF is essential to apply it as a preanalytical method that can be coupled online with MS analyzers, and for comprehensive applications in the areas of nanotechnology, proteomics and biotechnology. The limited availability of separation membranes suitable for the analysis of charged and neutral analytes both in organic and aqueous solvents still slightly restricts the exploitation of AsFlFFF. The recoveries, obtained e.g. for DNA complexes with cationic liposomes by using the current separation membranes are still below 70%. Hopefully new advances in membrane technology will provide products enabling high recoveries in a wide range of applications.

Acknowledgments

Financial support was provided by the Research Council for Natural Sciences and Engineering, the Academy of Finland under grants 116288 and 1133184 (M.-L.R.) and 122933 (Y.G. and K.H.).

References

[1] J.C. Giddings, Science 260 (1993) 1456.
[2] J.C. Giddings, Sep. Sci. 1 (1966) 123.
[3] M.N. Myers, J. Microcolumn Sep. 9 (1997) 151.
[4] M.R. Schure, M.E. Schimpf, P.D. Schettler, in: M.E. Schimpf, K.D. Caldwell, J.C. Giddings (Eds.), Field-flow Fractionation Handbook, Wiley-Interscience, New York, 2000 (Chapter 2).
[5] K.D. Caldwell, in: M.E. Schimpf, K.D. Caldwell, J.C. Giddings (Eds.), Field-flow Fractionation Handbook, Wiley-Interscience, New York, 2000 (Chapter 5).
[6] H. Colfen, M. Antonietti, Adv. Polym. Sci. 150 (2000) 67.
[7] S.K.R. Williams, D. Lee, J. Sep. Sci. 29 (2006) 1720.
[8] T. Kowalkowski, B. Buszewski, C. Cantado, F. Dondi, Crit. Rev. Anal. Chem. 36 (2006) 129.
[9] J. Chmelik, Proteomics 7 (2007) 2719.
[10] F.A. Messaud, R.D. Sanderson, J.R. Runyon, T. Otte, H. Pasch, S.K.R. Williams, Prog. Polym. Sci. 34 (2009) 351.
[11] B. Roda, A. Zattoni, P. Reschiglian, M.H. Moon, M. Mirasoli, E. Michelini, A. Roda, Anal. Chim. Acta 635 (2009) 132.
[12] J.C. Giddings, F.J. Yang, M.N. Myers, Science 193 (1976) 1244.
[13] S.K.R. Williams, in: M.E. Schimpf, K.D. Caldwell, J.C. Giddings (Eds.), Field-Flow Fractionation Handbook, Wiley-Interscience, New York, 2000 (Chapter 17).
[14] K.G. Wahlund, C.J. Giddings, Anal. Chem. 59 (1987) 1332.
[15] K.-G. Wahlund, A. Litzén, J. Chromatogr. 461 (1989) 73.
[16] A. Litzén, K.-G. Wahlund, J. Chromatogr. 476 (1989) 413.
[17] A. Litzén, K.-G. Wahlund, J. Chromatogr. 548 (1991) 393.
[18] A. Litzén, K.-G. Wahlund, Anal. Chem. 63 (1991) 1001.
[19] A. Litzén, J.K. Walter, H. Krischollek, K.-G. Wahlund, Anal. Biochem. 212 (1993) 469.
[20] K.D. Caldwell, in: G.B. Howard (Ed.), Modern Methods of Particle Size Analysis, A Wiley-Interscience Publication, John Wiley and Sons, New York, 1984, Chemical Analysis, vol. 73 (Chapter 7).
[21] M.R. Schure, B.N. Barman, J.C. Giddings, Anal. Chem. 61 (1989) 2735.
[22] M.D. Joe, in: M.E. Schimpf, K.D. Caldwell, J.C. Giddings (Eds.), Field-Flow Fractionation Handbook, Wiley-Interscience, New York, 2000 (Chapter 3).
[23] J.C. Giddings, Y.H. Yoon, K.D. Caldwell, M.N. Myers, M.E. Hovingh, Sep. Sci. 10 (1975) 447.
[24] J.C. Giddings, Unified Separation Science, Wiley, New York, 1991, pp. 210.
[25] J.C. Giddings, M.R. Schure, M.N. Myers, G.R. Velez, Anal. Chem. 56 (1984) 2099.
[26] P.S. Williams, S.B. Giddings, J.C. Giddings, Anal. Chem. 58 (1986) 2397.
[27] J.C. Giddings, M.R. Schure, Chem. Eng. Sci. 42 (1987) 1471.
[28] M.E. Moon, H. Kwon, I. Park, Anal. Chem. 69 (1997) 1436.
[29] H. Prestel, R. Niessner, U. Panne, Anal. Chem. 78 (2006) 6664.
[30] D. Kang, M.H. Moon, Anal. Chem. 76 (2004) 3851.
[31] S. Oh, D. Kang, S.-M. Ahn, R.J. Simpson, B.-H. Lee, M.H. Moon, J. Sep. Sci. 30 (2007) 1082.
[32] G. Yohannes, M. Sneck, S.J.O. Varjo, M. Jussila, S.K. Wiedmer, P.T. Kovanen, K. Öörni, M.-L. Riekkola, Anal. Biochem. 354 (2006) 255.
[33] D. Kang, S. Oh, S.-M. Ahn, B.-H. Lee, M.H. Moon, J. Proteome Res. 7 (2008) 3475.
[34] P. Reschiglian, D. Melucci, A. Zattoni, L. Mallo, M. Hansen, A. Kummerow, M. Miller, Anal. Chem. 72 (2000) 5945.
[35] L.J. Gimbert, K.N. Andrew, P.M. Haygarth, P.J. Worsfold, TrAC, Trends Anal. Chem. 22 (2003) 615.
[36] S. Cao, J. Pollastrini, Y. Jiang, Curr. Pharm. Biotechnol. 10 (2009) 382.
[37] S. Hupfeld, D. Ausbacher, M. Brandl, J. Sep. Sci. 32 (2009) 1465.
[38] S. Hupfeld, D. Ausbacher, M. Brandl, J. Sep. Sci. 32 (2009) 3555.
[39] R. Lang, L. Vogt, A. Zuercher, G. Winter, LCGC North America 27 (2009) 844.
[40] S.E. Shadle, R. Rostock, L. Bonfrisco, M.E. Schimpf, J. Liq. Chromatogr. Relat. Technol. 30 (2007) 1513.
[41] E. Alasonati, M.-A. Benincasa, V.I. Slaveykova, J. Sep. Sci. 30 (2007) 2332.
[42] Z. Wei, M. McEvoy, V. Razinkov, A. Polozova, E. Li, J. Casas-Finet, G.I. Tous, P. Balu, A.A. Pan, H. Mehta, M.A. Schenerman, J. Virol. Methods 144 (2007) 122.
[43] Y.P. Chuan, Y.Y. Fan, L. Lua, A.P.J. Middelberg, Biotechnol. Bioeng. 99 (2008) 1425.
[44] J.C. Giddings, G.-C. Lin, M.N. Myers, J. Liq. Chromatogr. 1 (1978) 1.
[45] A. Zattoni, E.L. Piccolomini, G. Torsi, P. Reschiglian, Anal. Chem. 75 (2003) 6469.
[46] A. Hawe, W. Friess, M. Sutter, W. Jiskoot, Anal. Biochem. 378 (2008) 115.
[47] D. Le Cerf, S. Simon, J.-F. Argillier, L. Picton, Anal. Chim. Acta 604 (2007) 2.
[48] C.W. Isaacson, D. Bouchard, J. Chromatogr. A 1217 (2010) 1506.
[49] P.L. Ma, M.D. Buschmann, F.M. Winnik, Biomacromolecules 11 (2010) 549.
[50] P. Reschiglian, A. Zattoni, B. Roda, L. Cinque, D. Parisi, A. Roda, F.D. -Piaz, M.H. Moon, B.R. Min, Anal. Chem. 77 (2005) 47.
[51] H. Lee, S.K.R. Williams, K.L. Wahl, N.B. Valentine, Anal. Chem. 75 (2003) 2746.
[52] D. Kang, S. Oh, P. Reschiglian, M.H. Moon, Analyst 133 (2008) 505.
[53] P. Reschiglian, M.H. Moon, J. Proteomics 71 (2008) 265.
[54] K.H. Kim, M.H. Moon, J. Proteome Res. 8 (2009) 4272.
[55] G. Yohannes, S.K. Wiedmer, J. Hiidenhovi, A. Hietanen, T. Hyötyläinen, Anal. Chem. 79 (2007) 3091.
[56] K.H. Kim, M.H. Moon, Anal. Chem. 81 (2009) 1715.
[57] U.S. Congress, Office of Technology Assessment, Biopolymers: Making Materials Nature's Way-Background Paper, OTA-BP-E-102, U.S. Government Printing Office, Washington, DC, September 1993.
[58] T. Tanaka (Ed.), Modern Methods in Polymer Research and Technology, Academic Press, San Diego, CA, USA, 2000.
[59] M. Quaglia, E. Machtejevas, T. Hennessy, K.K. Unger, HPLC Made to Measure, 2006, p. 383.
[60] T.M. Laue, W.F. Stafford III, Annu. Rev. Biophys. Biomol. Struct. 28 (1999) 75.
[61] J.P. Gabrielson, M.L. Brader, A.H. Pekar, K.B. Mathis, G. Winter, J.F. Carpenter, T.W. Randolph, J. Pharm. Sci. 96 (2007) 268.
[62] M. Gilar, U.D. Neue, J. Chromatogr. A 1169 (2007) 139.
[63] P.H. O'Farrell, J. Biol. Chem. 250 (1975) 4007.
[64] S.P. Radko, A. Chrambach, Electrophoresis 23 (2002) 1957.
[65] W.W.C. Quigley, N.J. Dovichi, Anal. Chem. 76 (2004) 4645.
[66] H. Thielking, W.-M. Kulicke, J. Microcolumn Sep. 10 (1998) 51.
[67] C.C. Hoppe, L.T. Nguyen, L.E. Kirsch, J.M. Wiencek, J. Biol. Eng. 2 (10) (2008) 1.
[68] V.N. Uversky, FEBS Lett. 514 (2002) 181.
[69] D.C. Rambaldi, A. Zattoni, P. Reschiglian, R. Colombo, E. De Lorenzi, Anal. Bioanal. Chem. 394 (2009) 2145.
[70] J.R. Silveira, G.J. Raymond, A.G. Hughson, R.E. Race, V.L. Sim, S.F. Hayes, B. Caughey, Nature 437 (2005) 257.
[71] J. Luo, M. Leeman, A. Ballagi, A. Elfwing, Z. Su, j.-C. Janson, K.-G. Wahlund, J. Chromatogr. A 1120 (2006) 158.
[72] J. Song, W.-S. Kim, Y.H. Park, E.K. Yu, D.W. Lee, Bull. Korean Chem. Soc. 20 (1999) 1159.
[73] B. Demeule, M.J. Lawrence, A.F. Drake, R. Gurny, T. Arvinte, BBA 1774 (2007) 146.
[74] A. Samontha, C. Nipattamanon, J. Shiowatana, A. Siripinyanond, J. Agric. Food Chem. 56 (2008) 8809.
[75] G. Yohannes, S.K. Wiedmer, M. Elomaa, M. Jussila, V. Aseyev, M.-L. Riekkola, Anal. Chim. Acta 675 (2010) 191.
[76] H. Lee, S.K.R. Williams, S.D. Allison, T.J. Anchordoquy, Anal. Chem. 73 (2001) 837.
[77] S.E. Harding, K.M. Vaarum, B.T. Stokke, O. Smidsroed, Adv. Carbohydr. Anal. 1 (1991) 63.
[78] R.A. Cave, S.A. Seabrook, M.J. Gidley, R.G. Gilbert, Biomacromolecules 10 (2009) 2245.
[79] H. Storz, K.J. Müller, F. Ehrhart, I. Gómez, S.G. Shirley, P. Gessner, G. Zimmermann, E. Weyand, V.L. Sukhorukov, T. Forst, M.M. Weber, H. Zimmermann, W.-M. Kulicke, U. Zimmermann, Carbohydr. Res. 344 (2009) 985.
[80] I. Colinet, V. Dulong, T. Hamaide, D. Le Cerf, L. Picton, Carbohydr. Polym. 75 (2009) 454.
[81] L. Pitkanen, M. Tenkanen, P. Tuomainen, Anal. Bioanal. Chem. 399 (2011) 1467.
[82] G. Modig, L. Nilsson, B. Bergenstahl, K.-G. Wahlund, Food Hydrocolloid 20 (2006) 1087.
[83] S.E. Bowen, D.A. Gray, C. Giraud, M. Majzoobi, C.E.M. Testa, L.A.B. Perez, S.E. Hill, J. Cereal Sci. 43 (2006) 275.
[84] C.C. Rojas, K.-G. Wahlund, B. Bergenståhl, L. Nilsson, Biomacromolecules 9 (2006) 1684.
[85] A. Rolland-Sabaté, P. Colonna, M.G. Mendez-Montealvo, V. Planchot, Biomacromolecules 8 (2007) 2520.
[86] A. Rolland-Sabate, S. Guilois, B. Jaillais, P. Colonna, Anal. Bioanal. Chem. 399 (2011) 1493.
[87] Z. Souguir, S. Roudesli, E. About-Jaude, D.Le Cerf, L. Picton, J. Colloid Interface Sci. 313 (2007) 108.
[88] S. Mao, C. Augsten, K. Mäder, T. Kissel, J. Pharm. Biomed. 45 (2007) 736.
[89] C. Augsten, K. Mäder, Int. J. Pharm. 351 (2008) 23.
[90] J.H. Kwon, E. Hwang, I.-H. Cho, M.H. Moon, Anal. Bioanal. Chem. 395 (2009) 519.
[91] A. Maleki, A.-L. Kjoeniksen, B. Nystrom, Macromol. Symp. 274 (2008) 131.
[92] C. Augsten, W. Knolle, K. Mäder, Carbohydr. Polym. 72 (2008) 707.
[93] J.C. Giddings, F.J. Yang, M.N. Myers, J. Virol. 21 (1977) 131.
[94] L.K. Pattenden, A.P.J. Middelberg, M. Niebert, D.I. Lipin, Trends Biotechnol. 23 (2005) 523.
[95] R.L. Garcea, L. Gissmann, Curr. Opin. Biotechnol. 15 (2004) 513.
[96] R. Lang, G. Winter, L. Vogt, A. Zurcher, B. Dorigo, B. Schimmele, Drug Dev. Ind. Pharm. 35 (2009) 83.
[97] A. Citkowicz, H. Petry, R.N. Harkins, O. Ast, L. Cashion, C. Goldmann, P. Bringmann, K. Plummer, B.R. Larsen, Anal. Biochem. 376 (2008) 163.
[98] D.I. Lipin, Y.P. Chuan, L.H.L. Lua, A.P.J. Middelberg, Arch. Virol. 153 (2008) 2027.
[99] L.d.F. Pease III, D.I.I. Lipin, D.-H. Tsai, M.l.R. Zachariah, L.H.L. Lua, M.J. Tarlov, A.P.J. Middelberg, Biotechnol. Bioeng. 102 (2009) 845.
[100] N.L. Setälä, J.M. Holopainen, J. Metso, S.K. Wiedmer, G. Yohannes, P.K.J. Kinnunen, C. Ehnholm, M. Jauhiainen, Biochemistry 46 (2007) 1312.
[101] D.C. Rambaldi, A. Zattoni, S. Casolari, P. Reschiglian, D. Roessner, C. Johann, Clin. Chem. 53 (2007) 2026.
[102] D.C. Rambaldi, P. Reschiglian, A. Zattoni, C. Johann, Anal. Chim. Acta 654 (2009) 64.
[103] R.N. Qureshi, W. Th Kok, P.J. Schoenmakers, Anal. Chim. Acta 654 (2009) 85.
[104] J. Witos, G. Cilpa, G. Yohannes, K. Öörni, P.T. Kovanen, M. Jauhiainen, M.-L. Riekkola, J. Sep. Sci. 33 (2010) 2528.
[105] V.P. Torchilin, Drug Discov. 4 (2005) 145.

[106] V.P. Torchilin, V. Weissig (Eds.), Liposomes, 2nd 34 edn., Oxford University Press, Oxford, UK, 2003, 396 pp.
[107] S. Hupfeld, H.H. Moen, D. Ausbacher, H. Haas, M. Brandl, Chem. Phys. Lipids 163 (2010) 141.
[108] S. Li, J. Nickels, A.F. Palmer, Biomaterials 26 (2005) 3759.
[109] M.V. Linden, K. Meinander, A. Hellel, G. Yohannes, M.-L. Riekkola, L.S.J. Butcher, T. Viitala, S.K. Wiedmer, Electrophoresis 29 (2008) 852.
[110] K. Jores, W. Mehnert, M. Drechsler, H. Bunjes, C. Johann, K. Mäder, J. Control. Release 95 (2004) 217.
[111] D. Pappas, K. Wang, Anal. Chim. Acta 601 (2007) 26.
[112] B.N. Barman, E.R. Ashwood, J.C. Giddings, Anal. Biochem. 212 (1993) 35.
[113] S. Saenton, H. Lee, Y.-S. Gao, J.F. Ranville, S.K.R. Williams, Sep. Sci. Technol. 35 (2000) 1761.
[114] P. Reschiglian, A. Zattoni, B. Roda, S. Casolari, M.H. Moon, J. Lee, J. Jung, K. Rodmalm, G. Cenacchi, Anal. Chem. 74 (2002) 4895.
[115] S.K. Cho, S.H. Shim, K.R. Park, S.-H. Choi, S. Lee, Anal. Bioanal. Chem. 386 (2006) 2027.
[116] B.P. Jackson, J.F. Ranville, A.L. Neal, Anal. Chem. 77 (2005) 1393.
[117] D. Kang, J.S. Yoo, M.O. Kim, M.H. Moon, J. Proteome Res. 8 (2009) 982.